PAPER • **OPEN ACCESS**

Thermal Hydraulic Fracturing Applying Cryogenic Freezing Technique

To cite this article: N Tarom *et al* 2019 *IOP Conf. Ser.: Mater. Sci. Eng.* **495** 012076

View the article online for updates and enhancements.

IOP ebooks™

Bringing you innovative digital publishing with leading voices to create your essential collection of books in STEM research.

Start exploring the collection - download the first chapter of every title for free.

This content was downloaded from IP address 124.207.82.166 on 18/09/2019 at 17:43

IOP Conf. Series: Materials Science and Engineering **495** (2019) 012076 doi:10.1088/1757-899X/495/1/012076

Thermal Hydraulic Fracturing Applying Cryogenic Freezing Technique

N Tarom[1], Muhammad Zain Rasheed[2], Shehan Khan[3] and M M Hossain[4] and Mohammad Sarmadivaleh[5]

[1]Department of Petroleum Engineering, Curtin University, Miri, Sarawak, Malaysia

[2,3,4,5]Department of Petroleum Engineering, Curtin University, Perth, Australia

[1]Nathan.tarom@curtin.edu.my

Abstract. The cryogenic thermal technique is used in this experimental study to provide a fundamental insight on the application of waterless fracturing techniques instead of water-based fracturing methods. The fracturing techniques in this study are captured applying axial and lateral strain gauges accompanied with Lab View software to record the crack initiation and propagation through conventional and unconventional synthetic rock samples. The experiments have been run under unconfined and confined pressure conditions. The investigations throughout of this laboratory study reveal the weakening of rock samples after being exposed to the cryogenic temperature. The experiments indicate a considerable reduction in the Young's Modulus and an increase in the Poisson's Ratio for rock samples exposed to the freezing temperature.

1. Introduction

Hydraulic fracturing is a technique applied in the oil and gas industry to form additional pathways enhancing the production of oil and gas from hydrocarbon reservoirs. Statistics show hydraulic fracturing technology has been widely useful in the completion of more than two million wells to improve the oil and gas production around the world since 1940 [1, 2]. That is also a technique of stimulation in tight formations, particularly for coalbed methane and shale reservoirs, where, due to the very low permeability and porosity of these kind of formations, oil and gas cannot be produced at economic rates under primary depletion. Therefore, hydraulic fracturing is used as a stimulation method for conventional and unconventional formations to form additional pathways improving the rate of fluid flow from reservoir into the wellbore [3].

In the process of hydraulic fracturing operation, water-base fracking fluid is conventionally used to create fractures into the formation of interest. That is implemented using high pressure pumps for injecting fracking fluids into the wellbore. This process will apply? enough hydraulic pressure on the face of the selected section of the wellbore to insert tensile stress. However, due to drawbacks of applied water on the formation such as increasing of near wellbore water saturation, reduction of relative permeability and pollution of aquifer; waterless fracturing techniques, if implementable, could reduce or eliminate the risks of well stimulation [4]. The aim of this study is to involve laboratory experiments to investigate the waterless cryogenic thermal shock fracturing technique in terms of well stimulation.

Content from this work may be used under the terms of the Creative Commons Attribution 3.0 licence. Any further distribution of this work must maintain attribution to the author(s) and the title of the work, journal citation and DOI.
Published under licence by IOP Publishing Ltd

2. Hydrocarbon Fracturing

Hydraulic fracturing is performed to create stresses on the face of the nominated section of the wellbore by using high pressure pumps to apply enough hydraulic pressure. The stimulated tensile stress breaks the formation in the form of fractures. Mixture of water and proppants (sand or ceramic beads) is a typical fracking fluid which creates highly conductive fractures and keeps the fractures open once the hydraulic pressure is released [5]. In recent investigations, it has been reported that 90% of produced gas and 70% of oil production undergo hydraulic fracturing techniques [1].

2.1. Water-Base Fluid Fracturing

Nowadays, hydraulic fracturing technology mainly relies on water-based fluids; because, water is readily available and inexpensive. However, vast amounts of problems might be experienced in the field as a result of applying water-based fracking fluid. For a typical fracking operation, massive amount of water is required which means that even an enormous resource such as water can become sparse if improperly managed. An investigation of using water for hydraulic fracturing by the EPA in 2013 showed that approximately 6,800 sources of drinking water, serving 8.6 million people around the world, were within one-mile from a hydraulically fractured well (EPA, 2015). Therefore, the technical and environmental issues associated with using water-based fracking fluids in the process of hydraulic fracturing may arise as following [6];

- Increase near wellbore skin damage.
- Reduction of gas phase relative permeability for tight gas reservoirs due to the increase of water saturation.
- Reduction of pore throat size in water sensitive formation, e.g. swelling of clay minerals.
- Water shortage.
- Cost related to disposing the recovered fluid.
- Pollution of surface water and underground aquifers.
- The lack of vertical fracture propagation control applying hydraulic fracturing.
- High frictional pressure loses around the wellbore.

2.2. Waterless Cryogenic Fracturing

In 1940, waterless fracturing technology has firstly been developed and tested to increase the formation conductivity near the well-bore. Nowadays, different waterless fracturing technologies such as oil-based, explosive, nitrogen, supercritical CO2 and cryogenic fracturing methods are applied to improve the oil and gas production from conventional and unconventional reservoirs. Applying these methods, some technical issues and the need for the vast amount of water to perform fracking operations will be eliminated [4].

Among the waterless fracturing techniques, cryogenic fracturing method with the idea that the warm formation rock in contact with very cold cryogenic fluid induces micro fractures orthogonal to the exposed surface. Nitrogen and CO2 are the most common cryogenic fracking fluid which has been applied to propagate fractures [7]. Comparing pros and cons of nitrogen and CO2, nitrogen is non-toxic, non-reactive and environmentally friendly, while CO2 is the main component in CCS (Carbon Capture & Storage) technology which is harmful for the environment.

Very cold cryogenic fluid contacts with hot reservoir rock which lead to form fractures at the contact point because of the thermal difference between fluid and rock. This mechanism is known as the principle of cryogenic fracturing which induces thermal stress instead of pressure stress utilized in water based fracking fluids.

Cryogenic thermal fracturing has been investigated throughout of comprehensive studies in [8], [9], [10] and [11]. Alqatahni et al. [8] performed both unconfined and confined experiments to investigate how cryogenic thermal shocks may affect the rock properties. Their laboratory results showed a decrease of 36% in breakdown pressure for a typical sample after exposing to flowing cryogenic liquefied nitrogen (LN). Figure 1 shows the post fracturing on the sample exposed to the cryogenic LN. Also, the decrease in samples' breakdown pressure were resulted through confined experiments; e.g., the

breakdown pressure decreased 61% for another concrete sample. Ultimately, the increase in rock permeability was concluded by Alqatahni et al. [8], Cha et al. [9], Zhao et al. [10] and Carpenter [11] throughout of different studies as a result of fracture creation through the process of cryogenic treatment.

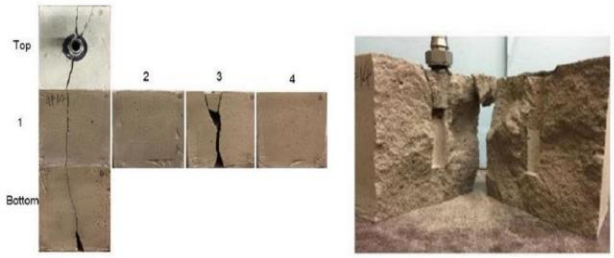

Figure 1. Sample 1 post fracturing [8].

3. Laboratory Experiments

3.1. Sample preparation

For the purposes of this study, synthetic samples were made to perform geo-mechanical experiments. The sandstone samples were made from a sand-cement ratio and water-cement ratio of 10 and 1.5, respectively [12]. Also, the ternary diagram of four Barnett shale wells in the United States [13] is used to prepare other synthetic samples. The red dot on Figure 2 shows the compositions of samples which are 10% carbonate, 30% silica and 60% kaolinite clay. For these samples, the ratio of water to the total weight of mixture was 1.25.

Sample were placed in an oven for the period of two weeks for the process of sample curing. Best samples (Figure 3) were selected considering that the specimens do not consist of any chipped edges, surface pore spaces or uneven surface. Samples also were trimmed to 1.5 in diameter and 3 in length using a mechanical saw (Figure 4) ensuring the both end of the samples were flat. This would ultimately improve the success rate of the geomechanical tests from problems that would arise due to instability.

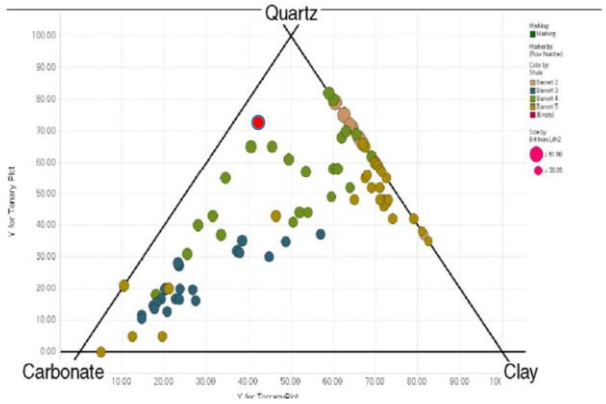

Figure 2. Composition of various shales in the Barnett [13].

Figure 3. Synthetic shale samples.

In this study, lateral and axial strain gauges positioned at the centre of samples were used to measure the applied stress on the samples (Figure 5). Strain gauges are formed from delicate strips of film with

a metallic foil pattern on the inside which measures the applied strains by detecting the change in electrical resistance as the foil is deformed.

Figure 4. Mechanical saw applied to flatten ends of samples.

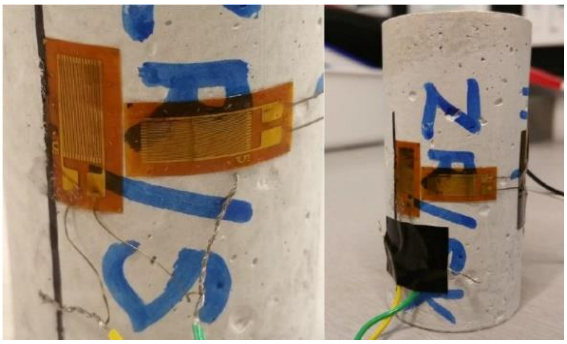

Figure 5. Samples with the axial and lateral strain gauges.

3.2. Perform experiments

The experiments were designed to record and compare the change of rock properties such as Young's modulus, Poisson's ratio and crack initiation at four different stress conditions. So, the experiments were performed at unconfined and confined pressure conditions for normal samples and the samples exposed to a thermal shock. To initiate the conditions, stress frame, hoke cell and syringe pumps are used to run the tests. Uniaxial compression tests (UCS) (Figure 6) were performed on four samples to measure the rock's compressive strength both for normal samples and the samples exposed to the thermal chock condition. These have been done by applying uniaxial load (vertical load) on cylindrical specimen without any confining stress.

Figure 6. Stress frame used to perform experiments.

The same experiments were run on another four samples both for normal samples and the samples exposed to the thermal chock condition except using hoke cell to create confined stress conditions (Figure 7).

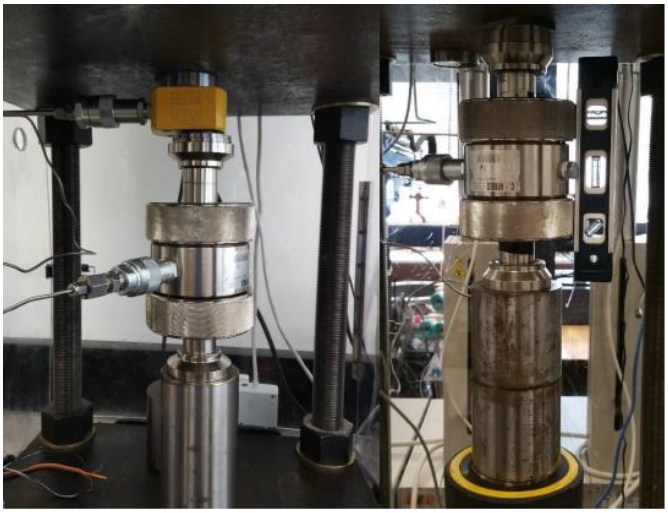

Figure 7. Stress frame plus hoke cell to insert confining pressure.

Equation (1) is used to calculate the compressive strength which is the force applied on the sample over a cross-sectional area.

$$\sigma_c = {}^{F}/_{A} \quad (1)$$

Where, A is the cross-sectional area and F represents the maximum force applied over the cross-sectional area.

3.3. Thermal Shocking Technique

Due to the safety concerns working with LN, initiation of thermal shocking stress using the combination of oven and dry ice was applied along these experimental investigations. To do that, five specimens were firstly placed in an oven at 50 degrees Celsius for 24 hours. After ensuring the temperature of every sample were homogenously at 50 °C, the samples were placed in a polystyrene insulated box and covered with dry ice at -80 °C. This was done to place the specimens in an environment with a huge temperature change from 50 to -78.5 degrees Celsius (almost 120 °C difference), to maximise the effect of thermal shocking.

Among the five samples exposed to the thermal shock, three samples were used for UCS test and two samples were applied for confining pressure experiments. A comparison between dry ice thermal properties and liquid nitrogen thermal properties can be seen on Table 1.

Table 1. Liquid nitrogen and dry ice thermal properties.

Property	Value	
	Dry Ice	N2
Molecular Weight	44	28
Density (kg/m^3)	1562	808
Specific Heat - cp	0.199	0.249
Specific Heat Ratio - cp/cv	1.3	1.4
Thermal Conductivity (Btu/hr ft oF)	0.009	0.015
Boiling Point (°C)	-78.5	-195.8

4. Laboratory results and discussion

The UCS test was performed on synthetic cylindrical samples (1.5 in diameter and 3 in height) by increasing the axial load at the rate of 50 psi/min using programmable ISCO syringe pumps until the samples failed. The raw outputs recorded using LabView software consist of time, axial stress, lateral stress and confining pressure. Young's modulus, the stiffness of a rock, is measured as the ratio of

longitudinal stress (force per unit area) divided by strain (proportional deformation). Lateral and axial strains are plotted against the axial stress. Equation 2 is also used to calculate Poisson's ratio (μ).

$$\mu = -{}^{\varepsilon_{lateral}}/_{\varepsilon_{axial}} \quad (2)$$

Where, $\mathcal{E}_{lateral}$ and $\mathcal{E}_{axial}$ are lateral and axial strains, respectively.

The test results of Young's modulus, Poisson's Ratio and UCS tests are summarized in Tables 2 and 3.

Table 2. Laboratory UCS test results before and after the exposure of samples to the thermal shock.

	Before			After		
	#1	#2	#3	#1	#2	#3
Young's Modulus (GPa)	5.17	3.58	5.21	6.44	2.92	4.17
Poisson's Ratio	0.17	0.10	0.12	0.11	0.16	0.21
UCS (MPa)	12.2	12.9	10.9	15.0	4.9	5.2

Table 3. Tri-axial test results before and after the exposure of samples to the thermal shock.

	Before		After	
	#4	#5	#4	#5
Young's Modulus (GPa)	4.14	4.19	3.16	2.03
Poisson's Ratio	0.12	0.12	0.15	0.06
UCS (MPa)	18.5	19.8	14.3	12
Confining Pressure (psi)	100	200	100	200

The failure UCS test results of samples #3 and #5 are also shown on Figures 8 and 9, respectively.

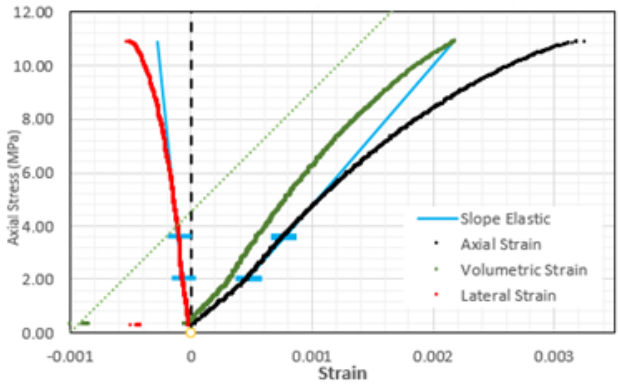

Figure 8. Sample #3 UCS test before and after thermal shock.

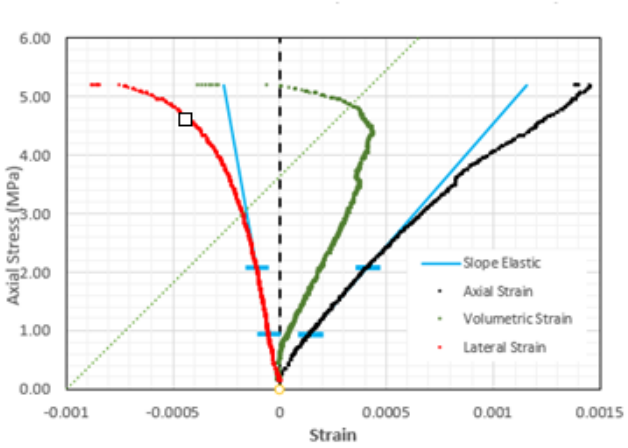

Figure 9. Sample #5 UCS test before and after thermal shock.

An investigation through the analysis of Mohr Coulomb failure envelope is performed to compare the effect of thermal shock temperature on the synthetic rock samples. In this analysis, $\sigma 3$ and $\sigma 1$ represent the confining stress (least principal stress) and the UCS value (maximum principal stress),

respectively. The Mohr Coulomb failure envelopes for both conditions, before and after the exposure of samples to the thermal shock temperature, are graphed on Figures 10 and 12, respectively.

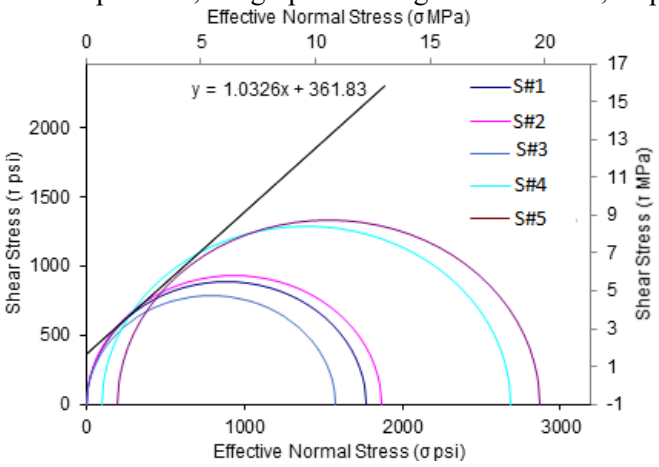

Figure 10. Mohr-Coulomb failure plane before thermal shock.

From the analysis of Figure 10, which is the Mohr Coulomb failure envelope for samples on Table 2 and 3 before exposure to the thermal shock, it can be said that the failure plane perfectly sits on five Mohr circles at different confining pressures. This indicates that all specimens obtained the consistent results. Figure 10 shows that the cohesion (C) is equal to 2.5MPa and consequently it can be evaluated that the internal friction angle (φ) is equal to 45.92°. In addition, the axial verses confining failure envelope follows a linear trend. The UCS value of 12.32MPa is obtained which is pretty close to the average measured value of 12.01MPa, obtained from the uniaxial tests.

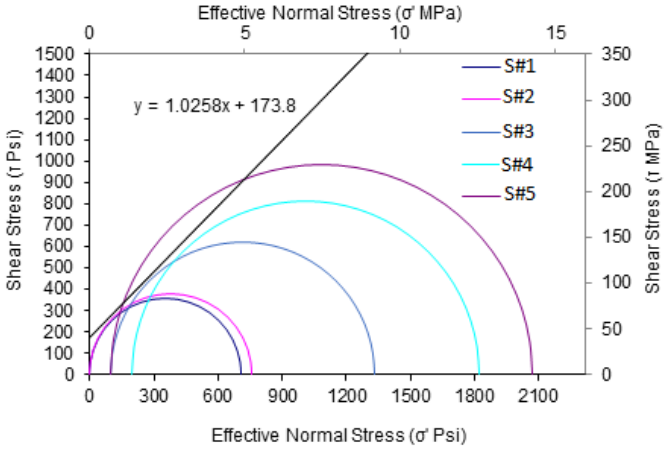

Figure 11. Mohr-Coulomb failure plane after thermal shock.

The same analysis has been done on Figure 11 which is the Mohr Coulomb failure envelope for samples on Table 2 and 3 after exposure to the thermal shock where samples were exposed to the thermal shock temperature. The consistent results can be seen from the Mohr circles. The evaluated internal friction angle (φ) and cohesion (C) are 45.73° and 1.20MPa, respectively. The R squared value obtained from axial verses confining failure envelope is 0.68 which follows a linear trend. From the liner trend, it can be obtained that the UCS value is 5.98MPa which is very similar to the average measured UCS value of 5.03MPa.

Ultimately, from the results obtained Figures 10 and 11, it is evident that rock's mechanical properties (Young's Modulus, UCS, confining compressive strength, shear strength and cohesion) for all specimens decreased after samples are being exposed to a thermal shock temperature.

5. Conclusion

A range of uniaxial and tri-axial tests were carried out to assess the elastic properties and failure characteristics of the synthetic shale and sand specimens before and after thermal chocking treatment. The results reveal that thermal shock treatment significantly decreases the rock's mechanical properties such as Young's Modulus, UCS, confining compressive strength, shear strength and cohesion. This study shows that the unconfined and confined compressive strength of the selected samples decreased by an average value of 53% and 50%, respectively. There is little to no change in the internal friction angle, while the cohesion decreased dramatically by 52% which means the Mohr-Coulomb failure plane shifted down by 52% after thermal shock treatment.

The changes in rock strength parameters and cohesion can be concluded from the mechanism of thermal stresses loaded on the samples. Long exposure to thermal shocking treatment may have resulted in the weakening of rock cementation and the creation of micro-cracks along the sample. This could also be due to the change in the size of the pre-existing flaws within the specimen. Ultimately, the results obtained from laboratory studies verifies that the effect of thermal shock treatment can alter the rock's mechanical properties.

References

[1] Wang L, Yao B, Cha M, Alqahtani N B, Patterson T W, Kneafsey Timothy J, Miskimins Jennifer L, Yin Xiaolong and Wu Y-S 2016 *Journal of Natural Gas Science and Engineering* **35** 160-174
[2] Coulter G R 1976 Hydraulic Fracturing - New Developments *JCPT* **15** 35-40
[3] Zhang B, Liu J, Wang S G, Li S, Yang X, Li Y, Zhu P and Yang W 2018 *Journal of Natural Gas Science and Engineering* **57** 155-165
[4] Rassenfoss S 2013 In Search of the Waterless Fracture *JPT* **65(6)** 46-52
[5] King S R 1983 Liquid CO2 for the Stimulation of Low-Permeability Reservoirs *SPE/DOE 11616* 145-151
[6] Cai C, Gao F, Li G, Huang Z and Hou P 2016 *Journal of Natural Gas Science and Engineering* **29** 30-36
[7] McDaniel B W, Grundmann S R, Kendrick W D, Wilson D R and Jordan S W 1997 Field Applications of Cryogenic Nitrogen as a Hydraulic Fracturing Fluid *SPE 38623* 561-572
[8] Alqatahni N B, Cha M, Yao B, Yin X, Kneafsey T J, Wang L, Wu Y-S and Miskimins J L 2016 *78th EAGE SPE Conf. and Exh.* (Vienna: Austria) SPE-180071-MS
[9] Cha M, Alqahtani N B, Yao B, Yin X, Kneafsey T J, Wang L, Wu Y-S, and Miskimins J L 2018 Cryogenic Fracturing of Wellbores Under True Triaxial-Confining Stresses: Experimental Investigation *J. of SPE* 1271-1289
[10] Zhao B, G Zhang, and Q Lin 2016 The Application of Cryogenic Treatment during Refracture Process - Laboratory Studies *50th U.S. Rock Mechanics/Geomechanics Symp. ARMA* (USA: Houston, Texas) ARMA 16-552
[11] Carpenter C 2017 Cryogenic-Fracturing Treatment of Synthetic-Rock With Liquid Nitrogen *JPT* doi:10.2118/0617-0070-JPT
[12] Younessi A, Rasouli V and B Wu 2012 Proposing a Sample Preparation Procedure for Sanding Experiments *Southern Hemisphere Inter. Rock Mech. Symp. SHIRMS*
[13] Rickman R, Mullen M J, Petre J E, Grieser W V and Kundert D 2008 A Practical Use of Shale Petrophysics for Stimulation Design Optimization: All Shale Plays Are Not Clones of the Barnett Shale *SPE* (USA: Denver, Colorado)